



Deposited via The University of Sheffield.

White Rose Research Online URL for this paper:

<https://eprints.whiterose.ac.uk/id/eprint/139341/>

Version: Accepted Version

Article:

Wang, Y., Feng, J.H., Guo, S.Y. et al. (2018) Investigation of optimal Split ratio for high-speed permanent-magnet brushless machines. IEEE Transactions on Magnetics, 54 (11). 8105605. ISSN: 0018-9464

<https://doi.org/10.1109/TMAG.2018.2841201>

© 2018 IEEE. Personal use of this material is permitted. Permission from IEEE must be obtained for all other users, including reprinting/ republishing this material for advertising or promotional purposes, creating new collective works for resale or redistribution to servers or lists, or reuse of any copyrighted components of this work in other works. Reproduced in accordance with the publisher's self-archiving policy.

Reuse

Items deposited in White Rose Research Online are protected by copyright, with all rights reserved unless indicated otherwise. They may be downloaded and/or printed for private study, or other acts as permitted by national copyright laws. The publisher or other rights holders may allow further reproduction and re-use of the full text version. This is indicated by the licence information on the White Rose Research Online record for the item.

Takedown

If you consider content in White Rose Research Online to be in breach of UK law, please notify us by emailing eprints@whiterose.ac.uk including the URL of the record and the reason for the withdrawal request.

Investigation of Optimal Split Ratio for High-Speed Permanent Magnet Brushless Machines

Y. Wang¹, J. H. Feng², S. Y. Guo², Y.F. Li², Z. C. Chen², Y. Wang², and Z. Q. Zhu¹, *Fellow, IEEE*

¹Department of Electronic and Electrical Engineering, University of Sheffield, Mappin Street, Sheffield S1 3JD, UK

²CRRC Zhuzhou Institute Co. Ltd, Shidai Road, Shifeng District, Zhuzhou, Hunan, 412001, China

The split ratio, i.e. the ratio of rotor outer diameter to stator outer diameter, is one of the most vital design parameters for PM machines due to its significant impact on the machine torque or power density. However, it has been optimized analytically in existing papers with due account only for the stator copper loss, which is reasonable for low to medium speed PM machines. For high speed PM machines (HSPMM), the negligence of stator iron loss and the mechanical stress on the rotor will lead to a deviation of optimal split ratio and actual torque capability. In this paper, the optimal split ratio of HSPMM is investigated analytically with the consideration of stator iron loss as well as the mechanical stress on the rotor. The influence of air gap length and rotor pole pairs on the optimal split ratio is elaborated. Both the analytical and finite element analysis reveal that the optimal split ratio for HSPMM will be significantly reduced when stator iron loss and mechanical constraints are taken into account.

Index Terms—high speed, iron loss, mechanical constraint, optimal split ratio, permanent-magnet machine.

I. INTRODUCTION

In the past few decades, permanent magnet brushless machines are among one of the most popular machines due to their high efficiency and compactness which are extremely desirable for high speed applications [1]-[3]. High speed PM machines (HSPMM) have been applied to a variety of applications such as domestic appliances, compressors, electrical turbo-compounding systems [4].

However, the inherent high speed and induced high frequency will also yield a huge centrifugal force and a significant electromagnetic loss in the rotor and stator. This two limitations impose a great constraint on the capability of power density and efficiency [5]-[6].

On the other hand, the split ratio of rotor outer diameter to stator outer diameter is one of the most important design parameters for HSPMM due to its significant impact on machine torque/power capability and efficiency. It has been optimized analytically for PM machines in existing papers. [7] derived a simple analytical expression of optimum split ratio for maximum torque density. In [8], the optimal split ratio of both brushless AC and DC motors having either overlapping or non-overlapping windings was further investigated. In addition, the influences of air gap flux density waveforms, stator tooth-tips as well as the end-winding on the optimal split ratio were discussed. In [9], the optimal split ratio as well as the flux density ratio were analyzed both individually and globally for fractional-slot IPM machine.

However, the boundary conditions are always restricted to a fixed copper loss or current density only, which is valid for low-to medium speed operating machines. For HSPMM, the stator iron loss resulting from the induced high frequency as well as the huge centrifugal stress on the rotor should also be considered. Neglecting these constraints will eventually lead to deviation of optimal split ratio and achievable power density.

In this paper, the optimal split ratio for HSPMM is obtained with the consideration of stator iron loss and mechanical constraints. The influence of design parameters such as air gap

length and rotor pole pairs on the optimal split ratio is investigated in detail. The analytical results are verified by the finite element analyses.

II. OPTIMAL SPLIT RATIO FOR HSPMM CONSIDERING STATOR IRON LOSS

Compared with low speed PM machines, the stator iron loss of HSPMM cannot be ignored due to the inherent high frequency. This iron loss can even be dominant for HSPMM operating at ultra-high speed (>100krpm). In this section, the optimal split ratio of HSPMM considering the stator iron loss will be investigated in detail.

Generally, a two-term iron loss model can be adopted for calculating the iron losses with the acceptable accuracy, while the classic loss and excess loss in the three-term model are combined into a global eddy current loss [10]-[12]. This model can be expressed as:

$$W_{Fe} = k_h f B_{Fe}^2 + k_e f^2 B_{Fe}^2 \quad (1)$$

where W_{Fe} denotes iron loss in watts per kilogram, k_e and k_h represent the hysteresis coefficient and eddy current coefficient, respectively. f denotes the frequency of magnetic field. B_{Fe} denotes the flux density in the stator iron.

On the other hand, the stator iron flux density can be expressed as:

$$B_{Fe} = \gamma B_g \quad (2)$$

where γ denotes the flux density ratio and B_g denotes the air gap flux density. Hence, the stator iron loss can be further written as:

$$P_{Fe} = W_{Fe} m_{Fe} = B_g^2 \gamma^2 \rho_{Fe} A_{Fe} l_a (k_h f + k_e f^2) \quad (3)$$

where ρ_{Fe} denotes the mass density of stator iron, A_{Fe} denotes the stator lamination area and l_a represents the stack length.

For the given machine frame size, the total heat transferred through the external surface depends on the specific cooling type. This heat source, namely electromagnetic loss can be written as [5]:

$$P_{limit} = h v_m \pi D_s l_a \quad (4)$$

where h denotes the thermal heat transfer coefficient and v_m denotes the maximum allowed temperature corresponding to specific insulation level. In HSPMM, the stator electromagnetic loss mainly consists of stator iron loss and winding copper loss. Thus, when the cooling type, stator outer diameter and stack length are given, the allowable stator copper loss can be expressed as:

$$P_{cu} = P_{limit} - P_{Fe} = P_{limit} - K_{Fe} A_{Fe} \quad (5)$$

where

$$K_{Fe} = B_g^2 \gamma^2 \rho_{Fe} l_a (k_h f + k_e f^2) \quad (6)$$

It can be seen that both stator iron loss and copper loss is closely related with the stator lamination area A_{Fe} which is determined by the split ratio, the stator teeth width and the back iron thickness. Fig.1 shows the structure of a typical HSPMM with 6s/4p-non-overlapping winding configuration. The permanent magnets are protected by the retaining sleeve in order to withstand the huge stress resulting from high speed. The specifications of the machine are given in Table I. Fig.2 illustrates the variation of stator iron loss and copper loss of a typical HSPMM with 6s/4p-Non-overlapping winding configuration. It can be seen that the stator iron loss becomes larger with the increase of split ratio before reaching the maximum value. The same trend is observed with the variation of iron area A_{Fe} when the stator flux density is constant. The stator iron area increases at the initial stage due to the wider teeth and yoke and then decreases as a result of smaller teeth height.

On the other hand, the stator copper loss is observed with the opposite trend to the stator iron loss when the total stator loss is fixed. It can be seen that the copper loss decreases with the increase of split ratio until reaching the minimum value. After this specific split ratio, the stator copper loss starts to increase mildly.

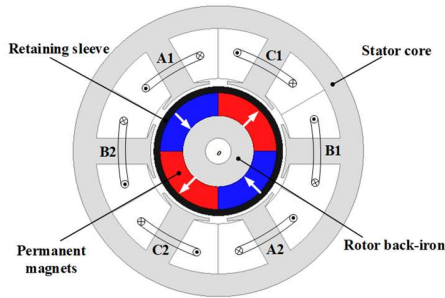


Fig. 1. Structure of a typical HSPMM.

TABLE I
SPECIFICATION OF HIGH SPEED PM MACHINE

Parameters		Parameters	
Stator outer diameter (mm)	90	Stator yoke thickness (mm)	4.4
Stator bore diameter (mm)	39.5	Stator teeth width (mm)	8.8
Split ratio	0.35	Packing factor	0.6
Rotor outer diameter (mm)	31.5	Stack axial length (mm)	55
Sleeve thickness (mm)	2	Number of turns per phase	20
PM thickness (mm)	8	Total stator loss (W)	200

In summary, when the stator iron loss is taken into consideration for HSPMM, the copper loss varies significantly with the split ratio instead of being constant. Therefore, the ampere turns will be directly affected due to the variation of copper loss. Hence, the variation of electromagnetic torque with

split ratio will be eventually altered. The torque expression for a three phase brushless PM motor can be derived as [8]:

$$T = \frac{3\sqrt{2}}{2} \sqrt{A_s} (\lambda D_o + 2g) \sqrt{\frac{P_{cu} k_s N_s l_a}{36 \rho_{cu}}} k_w B_g \quad (7)$$

where A_s denotes the slot area, λ denotes the split ratio which is defined as the ratio of rotor outer diameter and stator outer diameter. D_o is the stator outer diameter and g denotes the physical air gap length. k_s is the slot packing factor. N_s is the slot number and ρ_{cu} is the resistivity of copper. k_w represents the winding factor.

When (5) and (6) are substituted into (7), the electromagnetic torque can be further expressed as:

$$T = \frac{3\sqrt{2}}{2} k_w B_g \sqrt{\frac{k_s N_s l_a}{36 \rho_{cu}}} f(\lambda) \quad (8)$$

$$f(\lambda) = (D_o \lambda + 2g) \sqrt{A_s (p_{limit} - K_{Fe} A_{Fe})} \quad (9)$$

In (9), both A_s and A_{Fe} are functions of split ratio which have already been derived in [8]-[10]. Hence, the optimal split ratio for maximum electromagnetic torque considering stator iron loss can be obtained by solving the following differential as:

$$\frac{\partial f(\lambda)}{\partial \lambda} = 0 \quad (10)$$

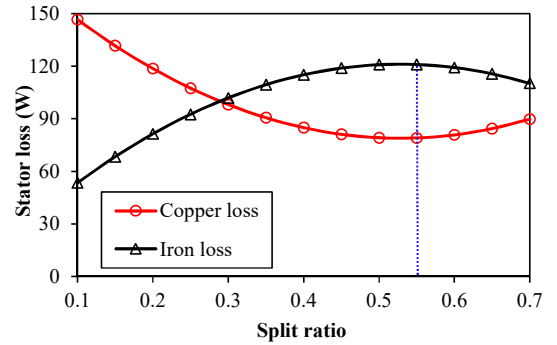


Fig. 2. Variation of stator loss with split ratio ($p=2$, $N_s=6$, $D_o=90$ mm, $P_{limit}=200$ W, $\gamma=0.5$, $f=2166$ Hz, $B_g=0.85$ T).

Fig.2 illustrates the electromagnetic torque versus split ratio with and without consideration of stator iron loss. It can be seen that the torque would be considerably reduced when the iron loss is taken into account. This should be attributed to the reduced copper loss thus electrical loading at each split ratio. In addition, the optimal split ratio for maximum electromagnetic torque has also been reduced due to the decreasing copper loss with the increasing split ratio before reaching minimum. The optimal split ratio has to be reduced in order to make the $f(\lambda)$ maximum.

It is worthy mentioning that torque variation range is relatively smaller when considering the stator iron loss. The electromagnetic torque decreases slowly after reaching the maximum value. As mentioned before, the copper loss turns to increase mildly which makes a compensation for the torque by increasing the electrical loading. Therefore, the electromagnetic torque will not drop sharply compared with that when only the copper loss is considered. As shown in Fig.3, although there is

a slight difference between the analytical and FE predicted torques, the optimal split ratios have a good agreement which verifies the validity of previous analytical analysis.

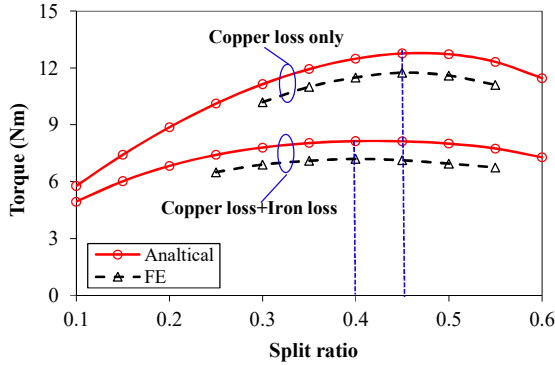


Fig. 3. Variation of electromagnetic torque with split ratio ($p=2$, $N_s=6$, $D_o=90\text{mm}$, $P_{\text{limit}}=200\text{W}$, $\gamma=0.5$, $f=2166\text{Hz}$, $B_g=0.85\text{T}$).

III. INFLUENCE OF DESIGN PARAMETERS ON OPTIMAL SPLIT RATIO

As mentioned in Section II, the optimal split ratio considering stator iron loss is closely related with the allowable copper loss variation trend versus split ratio. On the other hand, the design parameters affecting the variation of iron loss will pose the opposite impact on the allowable copper loss when the stator loss is fixed with certain cooling method. In this section, the influence of these design parameters such as air gap length as well as rotor pole pairs on the optimal split ratio will be elaborated.

A. Influence of air gap length on optimal split ratio

For HSPMM, the air gap length is relatively larger due to the presence of retaining sleeve. When the air gap length increases, the stator iron loss will be significantly decreased due to the reduced stator flux density. Thus, the allowable copper loss will be inversely increased as shown Fig.4. However, it changes little with the variation of split ratio when the air gap length becomes larger. This corresponds to the variation of stator iron loss with split ratio. As can be seen from (3), the stator iron loss depends on the stator flux density and the stator iron area when other parameters are constant. With the increase of air gap length, the stator iron loss increases more slowly due to the reduced stator flux density.

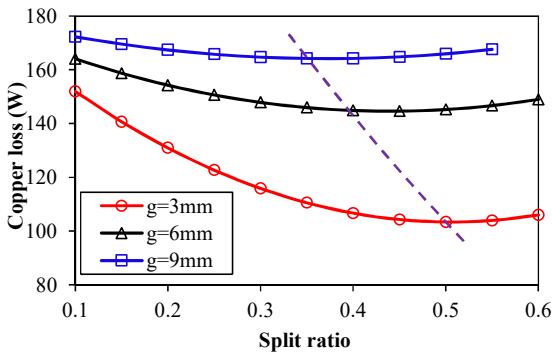


Fig. 4. Variation of copper loss with split ratio at different air gap length ($p=2$, $N_s=6$, $D_o=90\text{mm}$, $P_{\text{limit}}=200\text{W}$, $\gamma=0.5$, $f=2166\text{Hz}$).

Thus, with the increase of air gap length, the difference

between the optimal split ratios with and without consideration of stator iron loss decrease. As shown in Fig.5, when the air gap length reaches 9mm, the optimal split ratio almost remains constant as the copper loss changes little over the whole split ratio variation range.

However, the optimum split ratio of HSPMM considering stator iron loss will still decrease with increase of air gap length as shown in Fig.5. This can be attributed to the reduced slot area with the increasing air gap length. The optimum split ratio has to be reduced so that the total electromagnetic loss remains constant when the air gap length is relatively large.

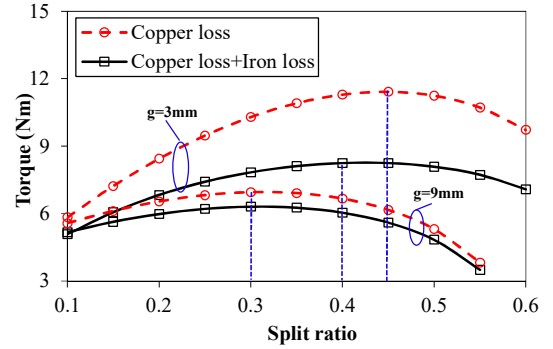


Fig. 5. Variation of electromagnetic torque with split ratio at different air gap lengths ($p=2$, $N_s=6$, $D_o=90\text{mm}$, $P_{\text{limit}}=200\text{W}$, $\gamma=0.5$, $f=2166\text{Hz}$).

B. Influence of rotor pole pairs on optimal split ratio

Compared with low-to-medium speed PM machines, the stator and rotor components of HSPMM, especially the permanent magnets are immersed in the high frequency variable magnetic field, yielding a significant amount of iron loss. A lower number of rotor pole pairs would not only contribute to the reduction of iron loss but also help to reduce switching loss in the inverters. Normally, the rotor pole pair of HSPMM is selected to be 1 or 2. In this section, the influence of rotor pole pairs of HSPMM on optimal split ratio is investigated.

Fig.6 illustrates the variation of stator loss with split ratio for the HSPMMs with 6s/4p-Non-overlapping and 6s/2p-Non-overlapping configuration. It is shown that the iron loss of HSPMM with 6s/2p-Non-overlapping configuration will be much smaller than that of 6s/4p-Non-overlapping due to half of the fundamental frequency. Hence, the allowable copper loss will be larger when the total electromagnetic loss is fixed. In addition, due to the smaller fundamental frequency, the iron loss of HSPMM with 6s/2p-Non-overlapping increase more mildly than that with 6s/4p-Non-overlapping. Accordingly, the allowable copper loss decreases gently with the increase of split ratio. Hence, the optimal split ratio for HSPMM with 6s/2p-Non-overlapping winding remains almost constant when the stator iron loss is taken into consideration. As has been proved, when the stator copper loss is considered only, the optimal split ratio will be reduced when the rotor pole pair decreases from 2 to 1 due to yoke thickness increase [8]. This reduction will be smaller when the stator iron loss is taken into account as shown in Fig.7. In other words, the optimal split ratio for HSPMM with 6s/2p-Non-overlapping is not as sensitive to the consideration of stator iron loss as 6s/4p-Non-overlapping configuration.

Although the allowable copper loss for 6s/2p-Non-overlapping is much larger, stator ampere turns are limited by the reduced slot area. More importantly, the winding factor of HSPMM with 6s/2p-Non-overlapping configuration is only 0.5, making the final electromagnetic torque significantly smaller than that of HSPMM with 6s/4p-Non-overlapping as shown in Fig. 7. It should be noted that the actual torque capability is still limited by the thermal constraints resulting from rotor eddy-current loss, especially for the HSPMM with 6s/4p-non-overlapping winding configuration. This will be further investigated in future.

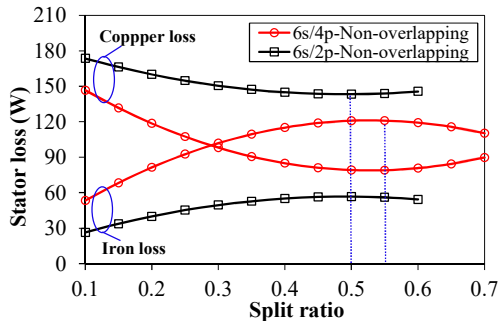


Fig. 6. Variation of stator loss with split ratio for different rotor pairs ($N_s=6$, $g=2\text{mm}$, $P_{\text{limit}}=200\text{W}$, $\gamma=0.5$).

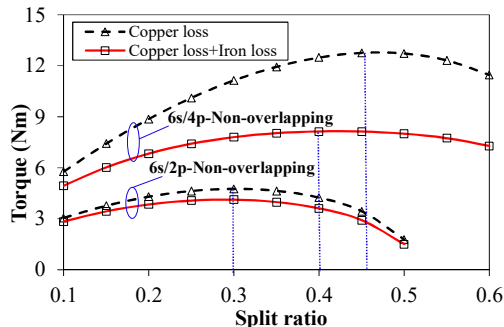


Fig. 7. Variation of electromagnetic torque with split ratio for different rotor pairs ($N_s=6$, $g=2\text{mm}$, $P_{\text{limit}}=200\text{W}$, $\gamma=0.5$).

IV. OPTIMAL SPLIT RATIO ACCOUNTING FOR MECHANICAL CONSTRAINTS

For HSPMM, at the preliminary design stage, it is important to take the mechanical constraints into consideration. Generally, two fundamental conditions should be satisfied: the tangential stress in the inner surface of sleeve should be within the material limits and the contact pressure between PM and rotor back-iron should be always positive [13].

When the mechanical constraints are taken into consideration, the stator flux density will be reduced due to the extra air gap length for retaining sleeve. As shown in Fig. 8, the minimum air gap length keeps increasing with the increase of split ratio. Hence, the limitation on air gap flux density becomes more severe with the enlarged air gap length. Accordingly, the stator iron loss will be reduced. In addition, the split ratio at which the stator iron loss reaches maximum is also decreased as shown in Fig. 9. This shift as well as the air gap flux density reduction will eventually lead to decrease of the optimal split ratio. Fig. 10 illustrates three curves of electromagnetic torque versus split ratio with respect to three different scenarios. It is

shown that optimal split ratio is significantly reduced when the stator iron loss and mechanical constraints are taken into consideration. Although the air gap flux density is reduced in the whole split ratio range, the restriction on the iron loss enables a larger allowable copper loss thus the electrical loading, eventually making the achievable electromagnetic torque almost constant when the mechanical constraints are taken into consideration.

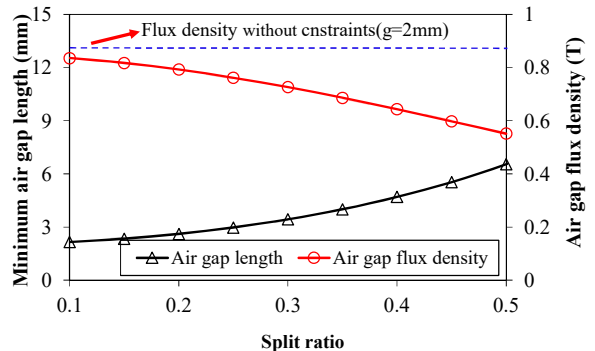


Fig. 8. Minimum air gap length and maximum flux versus split ratio with and without mechanical constraints ($N_s=6$, $g=2\text{mm}$, $n_{\text{max}}=120\text{krpm}$).

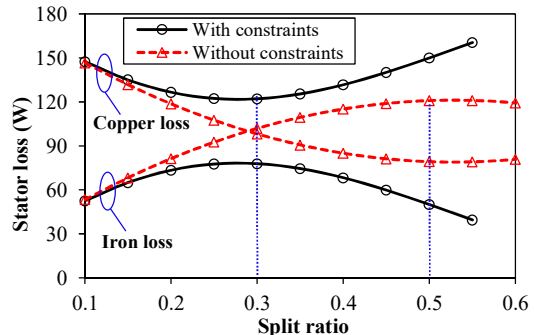


Fig. 9. Stator loss versus split ratio with and without mechanical constraints ($p=2$, $N_s=6$, $P_{\text{limit}}=200\text{W}$, $\gamma=0.5$).

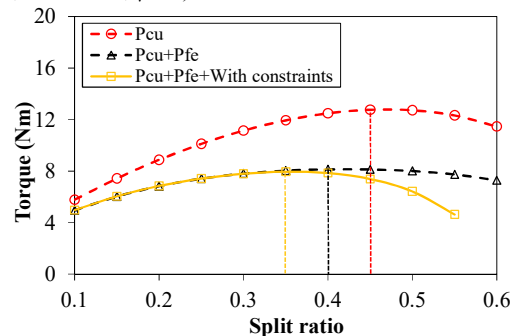


Fig. 10. Electromagnetic torque versus split ratio with different scenarios ($p=2$, $N_s=6$, $P_{\text{limit}}=200\text{W}$, $\gamma=0.5$).

V. CONCLUSION

In this paper, the optimal split ratio for HSPMM considering the stator iron loss as well as the mechanical constraints are analyzed analytically. The influence of design parameters including the air gap length and rotor pole pairs on the optimal split ratio is investigated in detail. Both the analytical and simulated results reveal that the optimal split ratio of HSPMM will be significantly reduced when the stator iron loss and mechanical constraints are taken into consideration.

REFERENCES

- [1] K. Ng, Z. Q. Zhu, and D. Howe, "Open-circuit field distribution in a brushless motor with diametrically magnetized PM rotor, accounting for slotting and eddy current effects," *IEEE Trans. Magn.*, vol. 32, pp. 5070–5072, Sept. 1997.
- [2] S.-M. Jang, H.-W. Cho, and S.-K. Choi, "Design and analysis of a high-speed brushless DC motor for centrifugal compressor," *IEEE Trans. Magn.*, vol. 43, no. 6, pp. 2573–2575, Jun. 2007.
- [3] D.-K. Hong, B.-C. Woo, J.-Y. Lee, and D.-H. Koo, "Ultra high speed motor supported by air foil bearings for air blower cooling fuel cells," *IEEE Trans. Magn.*, vol. 48, no. 2, pp. 871–874, Feb. 2012.
- [4] D. Gerada, A. Mebarki, N. L. Brown, C. Gerada, A. Cavagnino, and A. Boglietti, "High-speed electrical machines: technologies, trends, and developments," *IEEE Trans. Ind. Electron.*, vol. 61, no. 6, pp. 2946–2959, Jun. 2014.
- [5] N. Bianchi, S. Bolognani, and F. Luise, "Potentials and limits of high-speed PM motors," *IEEE Trans. Ind. Appl.*, vol. 40, no. 6, pp. 1570–1578, Nov./Dec. 2004.
- [6] K. Yamazaki and Y. Kato, "Optimization of high-speed motors considering centrifugal force and core loss using combination of stress and electromagnetic field analyses," *IEEE Trans. Magn.*, vol. 49, no. 5, pp. 2181–2184, May 2013.
- [7] F. B. Chaaban, "Determination of the optimal rotor/stator diameter ratio of permanent magnet machines," *Elect. Mach. Power Syst.*, vol. 22, pp. 521–531, 1994.
- [8] Y. Pang, Z. Q. Zhu, and D. Howe, "Analytical determination of optimal split ratio for permanent magnet brushless motors," *IEE Proc. Elect. Power Appl.*, vol. 153, pp. 7–13, Jan. 2006.
- [9] L. J. Wu, Z. Q. Zhu, J. T. Chen, Z. P. Xia, and G. W. Jewell, "Optimal split ratio in fractional-slot interior permanent-magnet machines with non-overlapping windings," *IEEE Trans. Magn.*, vol. 46, no. 5, pp. 1235–1242, May 2010.
- [10] A. Boglietti, A. Cavagnino, M. Lazzari, and M. Pastorelli, "Predicting iron losses in soft magnetic materials with arbitrary voltage supply: An engineering approach," *IEEE Trans. Magn.*, vol. 39, no. 2, pp. 981–989, Mar. 2003.
- [11] D. Lin, P. Zhou, W. N. Fu, Z. Badics, and Z. J. Cendes, "A dynamic core loss model for soft ferromagnetic and power ferrite materials in transient finite element analysis," *IEEE Trans. Magn.*, vol. 40, no. 2, pp. 1318–1321, Mar. 2004.
- [12] D. M. Ionel, M. Popescu, and S. J. Dellinger, "Computation of core losses in electrical machines using improved models for laminated steel," *IEEE Trans. Ind. Appl.*, vol. 43, no. 6, pp. 1554–1564, Nov./Dec. 2007.
- [13] A. Binder, T. Schneider, and M. Klohr, "Fixation of buried and surface-mounted magnets in high-speed permanent-magnet synchronous machines," *IEEE Trans. Ind. Appl.*, vol. 42, no. 4, pp. 1031–1037, Jul./Aug. 2006.